Trace Metals as Biomarkers for Eumelanin Pigment in the Fossil Record

R. A. Wogelius *et al.*

Science **333**, 1622 (2011);
DOI: 10.1126/science.1205748

Science (print ISSN 0036-8075; online ISSN 1095-9203) is published weekly, except the last week in December, by the American Association for the Advancement of Science, 1200 New York Avenue NW, Washington, DC 20005.

(*10*). These were probably borne by an animal capable of flight. Within UALVP 52820, barbules of unequal lengths arise from either side of the barb, producing a differentiated series of longer proximal (~0.42 mm) and shorter distal (~0.24 mm) elements, all having spinose nodal projections. Barbules are widely spaced along a thick ramus (barb shaft) adapted for rigidity and are strongly differentiated to interlock with adjacent barbs to form a vane (*10*).

On the basis of the presence of a rachis in TMP 96.9.334 and differentiated barbules in UALVP 52820, these specimens can be assigned conservatively to stages IV and V and are attributed to Late Cretaceous birds. The remaining six feathers are fragmentary downy and contour feathers (Fig. 3). Although they offer limited insight concerning the identity or behavior of their bearer, their structure and pigmentation bear directly on feather evolutionary stages. Four of the six feather fragments in TMP 96.9.997 (Fig. 3, A to D, and fig. S9) are aligned. Superficially, these exhibit an intermediate morphology (stage IIb) proposed for an Early Cretaceous (late Albian) French amber specimen (*4*). In the Canadian specimens, as in the French material, the main axis preserved is short (3.7 mm) and weakly defined, dorsoventrally flattened, and composed of fused secondary branches in an opposite arrangement. However, in the Canadian specimens intense pigmentation in each internode produces a beaded appearance, highlighting segmentation that is otherwise difficult to discern based on barbule diameter variation (Fig. 3C). Segmentation identifies the finest branches as barbules attached to narrow rami, and not barb equivalents attached to a rachis. This interpretation identifies these small specimens as subcomponents of a larger feather, such as basal barbs on a contour feather (*17*), and not a distinct stage in feather evolution lacking barbules (*4*). This interpretation probably extends to the French material as well. Pigmentation is preserved with fidelity in all additional specimens. Although downy feathers are consistently transparent, and would have been white in life, pennaceous feathers are more variable, with diffuse, transparent, and mottled patterns of pigmentation (Fig. 3, E to L) that match those observed in modern birds (*10*, *24*, *25*).

Although neither avian nor dinosaurian skeletal material has been found in direct association with amber at the Grassy Lake locality, fossils of both groups are present in adjacent stratigraphic units. Hadrosaur footprints are found in close association with the amber, and younger (late Campanian and Maastrichtian) strata of western Canada contain diverse nonavian dinosaur (*26*) and avian (*27*, *28*) remains. There is currently no way to refer the feathers in amber with certainty to either birds or the rare small theropods from the area (*26*). However, the discovery of end-members of the evolutionary-developmental spectrum in this time interval, and the overlap with structures found only in nonavian dinosaur compression fossils, strongly suggests that the protofeathers described here are from dinosaurs and not birds. Given that stage I filaments were present in densities relevant for thermoregulation and protection, and that comparable structures are preserved as coronae surrounding compression fossils, it becomes apparent that protofeathers had important nonornamental functions. Specialized barbule morphologies, including basal coiling, suggest that Campanian feather-bearers had already evolved highly specialized structures similar to those of modern grebes to enhance diving efficiency.

Canadian amber provides examples of stages I through V of Prum's (*11*) evolutionary-developmental model for feathers. None of the additional morphotypes observed in compression fossils of nonavian dinosaurs (*8*, *15*) or amber (*4*) were found here, suggesting that some morphotypes may not represent distinct evolutionary stages, or may not have persisted into the Late Cretaceous. The snapshot of Campanian feather diversity from Canadian amber is biased toward smaller feathers, subcomponents of feathers, feathers that are molted frequently, and feathers in body positions that increase their likelihood of contacting resin on tree trunks. Despite these limitations, the assemblage demonstrates that numerous evolutionary stages were present in the Late Cretaceous, and that plumage already served a range of functions in both dinosaurs and birds.

References and Notes

1. P. G. Davis, D. E. G. Briggs, *Geology* **23**, 783 (1995).
2. D. Schlee, W. Glöckner, *Stuttg. Beitr. Naturkd. C* **8**, 1 (1978).
3. J. Alonso *et al.*, *J. Paleontol.* **74**, 158 (2000).
4. V. Perrichot, L. Marion, D. Néraudeau, R. Vullo, P. Tafforeau, *Proc. Biol. Sci.* **275**, 1197 (2008).
5. D. Grimaldi, G. R. Case, *Am. Mus. Novit.* **3126**, 1 (1995).
6. Q. Ji, P. J. Currie, M. A. Norell, S.-A. Ji, *Nature* **393**, 39 (1998).
7. M. Norell, X. Xu, *Annu. Rev. Earth Planet. Sci.* **33**, 277 (2005).
8. X. Xu, Y. Guo, *Vertebrata PalAsiatica* **47**, 311 (2009).
9. R. C. McKellar, A. P. Wolfe, in *Biodiversity of Fossils in Amber from the Major World Deposits*, D. Penney, Ed. (Siri Scientific Press, Manchester, 2010), pp. 149–166.
10. Materials and methods are available as supporting material on *Science* Online.
11. R. O. Prum, *J. Exp. Zool.* **285**, 291 (1999).
12. R. O. Prum, A. H. Brush, *Q. Rev. Biol.* **77**, 261 (2002).
13. A. H. Brush, *Am. Zool.* **40**, 631 (2000).
14. P. J. Currie, P.-J. Chen, *Can. J. Earth Sci.* **38**, 1705 (2001).
15. X. Xu, X. Zheng, H. You, *Nature* **464**, 1338 (2010).
16. P. Stettenheim, *Living Bird* **12**, 201 (1973).
17. A. M. Lucas, P. R. Stettenheim, *Avian Anatomy: Integument* (U.S. Department of Agriculture, Washington, DC, 1972).
18. P.-J. Chen, Z.-M. Dong, S.-N. Zhen, *Nature* **391**, 147 (1998).
19. A. W. A. Kellner *et al.*, *Proc. Biol. Sci.* **277**, 321 (2010).
20. X. Xu, Z.-H. Zhou, R. O. Prum, *Nature* **410**, 200 (2001).
21. T. J. Cade, G. L. Maclean, *Condor* **69**, 323 (1967).
22. G. L. MacLean, *Bioscience* **33**, 365 (1983).
23. J. Fjeldså, *The Grebes: Podicipedidae* (Oxford Univ. Press, New York, 2004).
24. A. C. Chandler, *Univ. Calif. Publ. Zool.* **13**, 243 (1916).
25. C. J. Dove, *Ornith. Mono.* **51**, 1 (2000).
26. P. J. Currie, in *Dinosaur Provincial Park: A Spectacular Ancient Ecosystem Revealed*, P. J. Currie, E. B. Koppelhus, Eds. (Indiana Univ. Press, Bloomington, 2005), pp. 367–397.
27. N. Longrich, *Cretac. Res.* **30**, 161 (2009).
28. E. Buffetaut, *Geol. Mag.* **147**, 469 (2010).

Acknowledgments: We thank the Leuck family and M. Schmidt (donated specimens); M. Caldwell, S. Ogg and M. Srayko (microscopy); E. Koppelhus and H. Proctor (discussions); and J. Gardner, B. Strilisky, A. Howell, and J. Hudon (TMP, Redpath Museum, and Royal Alberta Museum collections). Research was funded by Natural Sciences and Engineering Research Council of Canada (NSERC) Discovery Grants to B.D.E.C., A.P.W., and P.J.C. and NSERC and Alberta Ingenuity Fund support to R.C.M.

Supporting Online Material

www.sciencemag.org/cgi/content/full/333/6049/1619/DC1
Materials and Methods
SOM Text
Figs. S1 to S12
References (*29*–*49*)

25 January 2011; accepted 22 July 2011
10.1126/science.1203344

Trace Metals as Biomarkers for Eumelanin Pigment in the Fossil Record

R. A. Wogelius,[1,2]* P. L. Manning,[1,2,3] H. E. Barden,[1,2] N. P. Edwards,[1,2] S. M. Webb,[4] W. I. Sellers,[5] K. G. Taylor,[6] P. L. Larson,[1,7] P. Dodson,[3,8] H. You,[9] L. Da-qing,[10] U. Bergmann[11]

Well-preserved fossils of pivotal early bird and nonavian theropod species have provided unequivocal evidence for feathers and/or downlike integuments. Recent studies have reconstructed color on the basis of melanosome structure; however, the chemistry of these proposed melanosomes has remained unknown. We applied synchrotron x-ray techniques to several fossil and extant organisms, including *Confuciusornis sanctus*, in order to map and characterize possible chemical residues of melanin pigments. Results show that trace metals, such as copper, are present in fossils as organometallic compounds most likely derived from original eumelanin. The distribution of these compounds provides a long-lived biomarker of melanin presence and density within a range of fossilized organisms. Metal zoning patterns may be preserved long after melanosome structures have been destroyed.

Feather color in birds stems mostly from chemical pigments, of which the most widely used are melanins (*1*). Resolving color patterns in extinct species may hold the key to understanding selection processes that acted during crucial evolutionary periods and

[1]School of Earth, Atmospheric, and Environmental Sciences, University of Manchester, Manchester M13 9PL, UK. [2]Williamson Research Centre for Molecular Environmental Science, University of Manchester, Manchester M13 9PL, UK. [3]Department of Earth and Environmental Sciences, University of Pennsylvania, Philadelphia, PA 19104, USA. [4]SLAC National Accelerator Laboratory, Stanford Synchrotron Radiation Lightsource (SSRL), Menlo Park, CA 94025, USA. [5]Faculty of Life Sciences, University of Manchester, Manchester M13 9PT, UK. [6]School of Science and the Environment, Manchester Metropolitan University, Manchester M1 5GD, UK. [7]Black Hills Institute of Geological Research, Hill City, SD 57745, USA. [8]School of Veterinary Medicine, University of Pennsylvania, Philadelphia, PA 19104, USA. [9]Chinese Academy of Geological Sciences, Institute of Geology, 26 Baiwanzhuang Road, Beijing, P. R. China, 100037. [10]Gansu Geological Museum, 6 Tuan Jie Road, Lanzhou, Gansu, P. R. China, 730030. [11]SLAC National Accelerator Laboratory, Linac Coherent Light Source, Menlo Park, CA 94025, USA.

*To whom correspondence should be addressed. E-mail: roy.wogelius@manchester.ac.uk

also may help discern nonflight functions such as camouflage, communication, and sexual selection.

Confuciusornis sanctus (Jehol Group, Lower Cretaceous, 131 to 120 million years ago) and *Gansus yumenensis* (Xiagou Formation, Lower Cretaceous, 115 to 105 million years ago) occupy key positions in the evolution of Aves; *C. sanctus* is the oldest documented species to display the derived avian beak (*2*), and *G. yumenensis* has been identified as the most ancient of the Ornithurae, the phylogenetic grouping that includes modern birds (*3*). Previous studies of similar material (*4*, *5*) suggested the presence of melanosomes and tentatively reconstructed feather colors. These studies used melanosome shape to extrapolate color; rod shapes were interpreted as eumelanosomes (dark black/brown), and spheroidal shapes as pheomelanosomes (reddish-brown). Other pigments (such as carotenoids) in feathers and physical structures besides melanosomes may contribute to color. Melanin granule morphology may vary among different species (*6*, *7*), and structural preservation may not be uniform. Therefore, color interpretation based solely on fossilized melanosome morphology and distribution has limitations (*4*, *5*, *8*).

Despite these additional complicating factors in color restoration, detailed chemical analysis of fossil material may make it possible to resolve remnants of pigmentation. In particular, a number of biologically important metal ions (such as Ca^{2+}, Cu^{2+}, Co^{2+}, and Zn^{2+}) are chelated by and affect the chemical properties of melanin (*1*, *9*–*11*) so that trace metal distributions are able to provide a chemical image of melanin distribution in extant feathers (*12*).

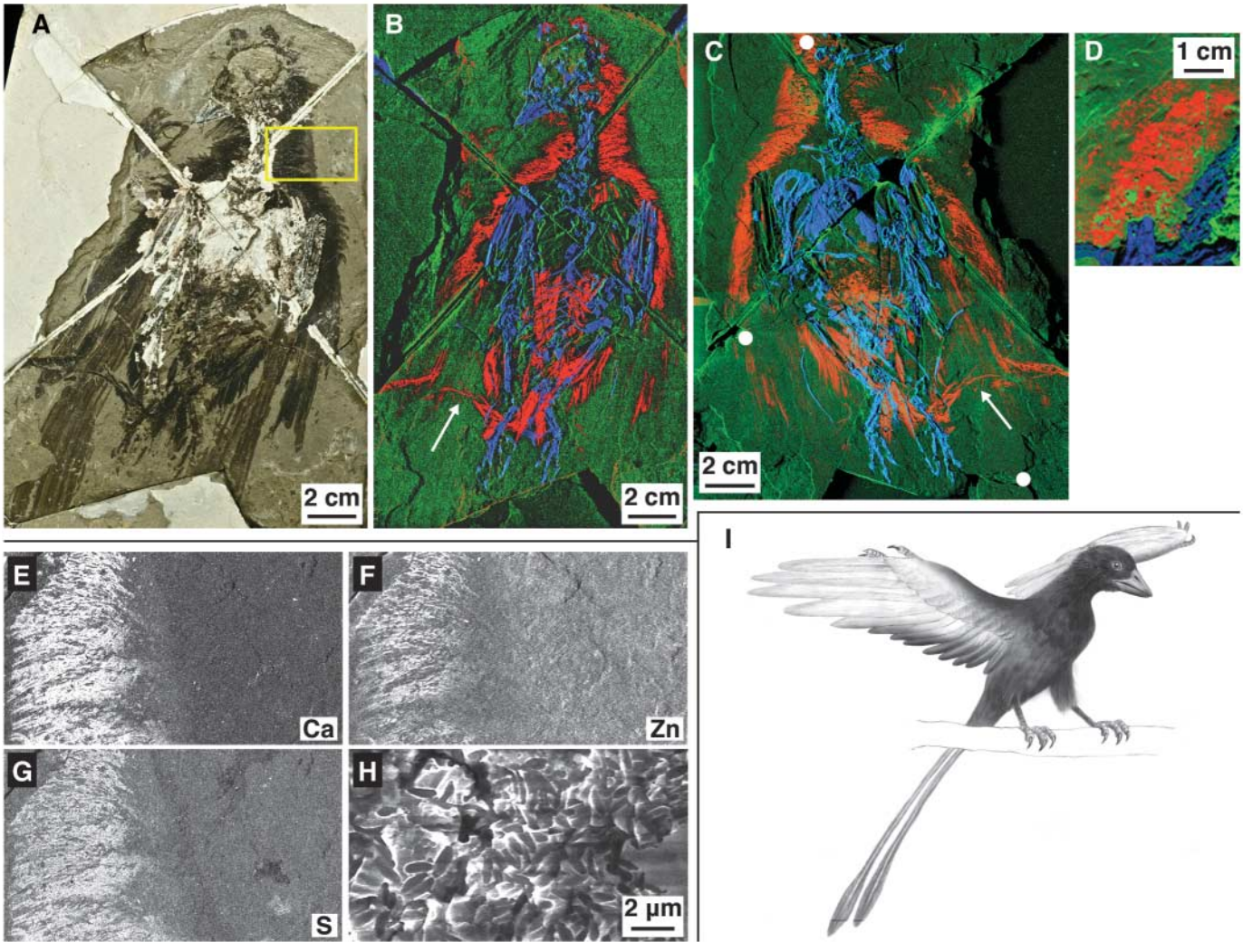

Fig. 1. (**A**) *C. sanctus* (MGSF315), optical image. Yellow box shows detailed neck region discussed below. (**B** and **C**) SRS-XRF false-color images of MGSF315 main slab and counterpart (red, Cu; blue, Ca; green, Zn). (**D**) Neck region SRS-XRF false-color image of a second *C. sanctus* (LL12418). (**E** to **G**) Single-element SRS-XRF maps of the main slab neck region of MGSF315 for (E) Ca, (F) Zn, and (G) S. (**H**) VP-FEG-SEM micrograph of possible eumelanosomes correlated with copper in the neck of MGSF315. (**I**) Artist's conception of eumelanin density in *C. Sanctus* based on the SRS-XRF images. Retrices in MGSF315 are folded; see white arrows in (B) and (C). White circles in (C) show SEM sample points.

Therefore, because of their non-biodegradability and the biocide properties of some metals, this may also be the case in fossils. Assuming trace metal distributions correlate with proposed melanosomes, a true chemical test would be to determine whether organic compounds (especially organometallic chelates) with an affinity to precursor melanin can be identified.

We applied chemical imaging to search for trace metal patterns in an exceptionally preserved specimen of *C. sanctus* (MGSF315), a lone feather of *G. yumenensis* (MGSF317), and several comparable fossil and extant samples, including the holotype of *Archaeopteryx lithographica* (*13*). Chemical analysis of fossils without destructive sampling is challenging, but recently synchrotron rapid-scanning x-ray fluorescence (SRS-XRF) has been successfully developed to fully map trace element distributions in large specimens that could not be observed with traditional methods (*14*). Extended x-ray absorption fine structure (EXAFS) and x-ray absorption near-edge structure (XANES) spectroscopies were used to probe the local structure of the mapped trace metals in order to determine whether they are likely to be derived from endogenous organic compounds. Variable pressure–field emission gun–scanning electron microscopy (VP-FEG-SEM) was used to compare trace element maps with fossil microstructure, and infrared spectroscopy was used to corroborate the EXAFS and XANES.

SRS-XRF maps of *C. sanctus* specimen MGSF315 (Fig. 1A) and its counterpart reveal several correlations between chemical distributions and structural features. False-color SRS-XRF images of Cu, Ca, and Zn data show that Cu is distinctly concentrated within the downy body feathers and also appears as discrete elongated patches within areas of the flight feathers (Fig. 1B). The characteristic *C. sanctus* retrices (tail feathers) can also be resolved in the copper map. Calcium (Fig. 1 B, blue) is high in bone, as would be expected, and zinc (Fig. 1 B, green) is distributed throughout the sedimentary rock at levels higher than copper. The counterpart slab mirrors the zonation pattern, indicating that the mapped metal distributions are reproducible and, more importantly, that the Cu distribution shown in Fig. 1B is not a partial chemical remnant caused by unevenly splitting the Cu inventory between two opposite slabs. A second *C. sanctus* specimen (LL12418) was mapped via SRS-XRF and also showed high Cu in the neck feathers (Fig. 1D). In birds that produce melanin, keratin may apparently chelate available Cu (*15*), or traces of tyrosinase may be entrained during feather growth so that Cu alone, despite its strong association with melanin production, should not solely be relied on as an indicator of melanin-based pigmentation. Calcium, Zn, Fe, and Mn are also typically associated with melanin pigmentation (*12*, *16*). SRS-XRF maps of Ca (Fig. 1E) and Zn (Fig. 1F) in the downy feathers of the *C. sanctus* (MGSF315) neck region show strong correlations with Cu and with each other (figs. S1 to S3 and table S1). Sulfur is a major component of feathers [~7 weight percent (wt %)], and S maps also correlate with divalent trace metals (Fig. 1G). Iron and Mn concentrations are so high in the sedimentary matrix that they obscure any patterning that might be present in the feather regions; however, the observed correlation of Cu, Ca, and Zn within S-bearing soft-tissue regions implies that there is a melanin-chelate–derived control on trace metal distribution in *C. sanctus* feathers.

VP-FEG-SEM imaging and chemical analysis of three ~1-mm-sized flakes from the coun-

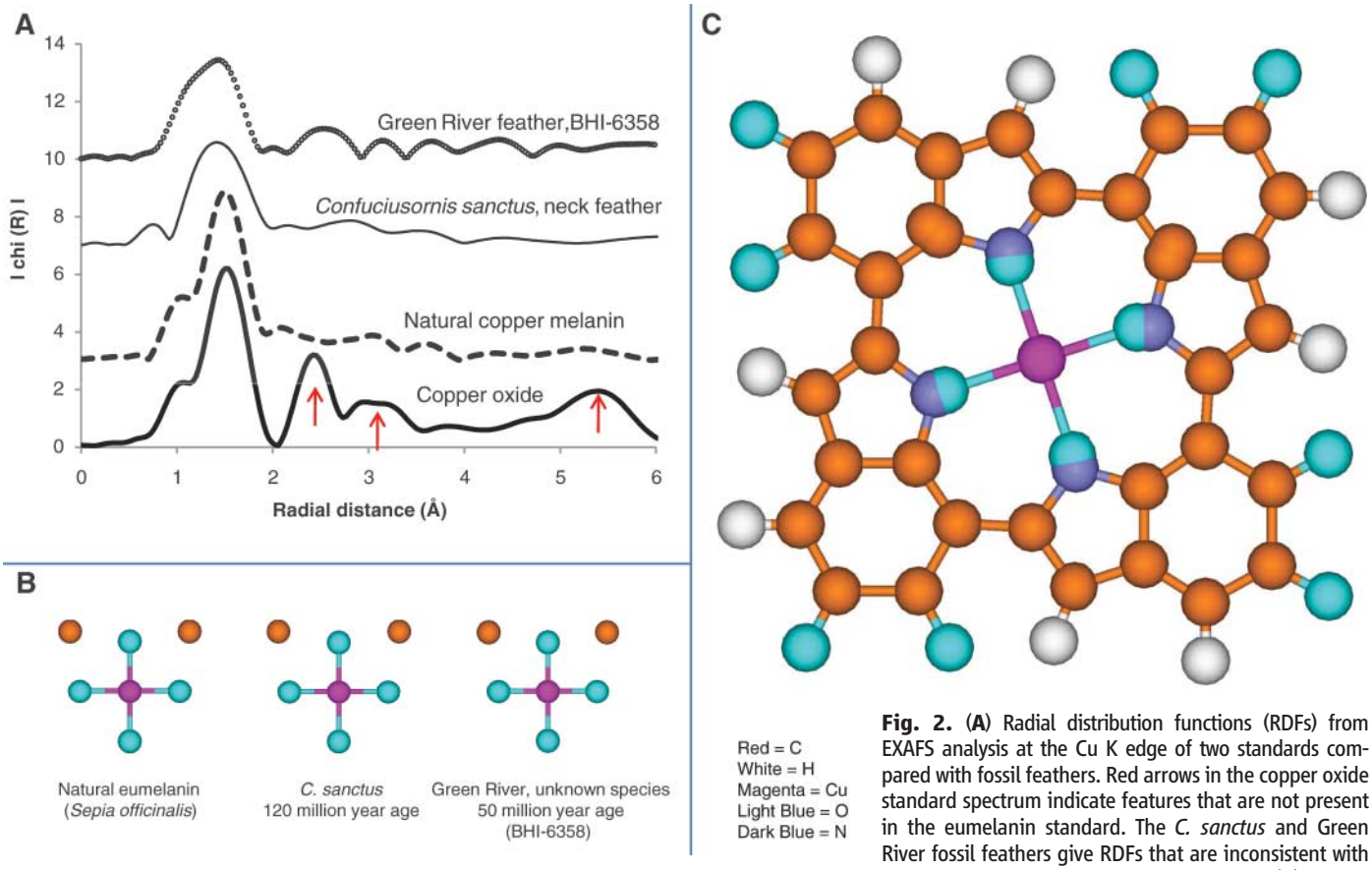

Fig. 2. (**A**) Radial distribution functions (RDFs) from EXAFS analysis at the Cu K edge of two standards compared with fossil feathers. Red arrows in the copper oxide standard spectrum indicate features that are not present in the eumelanin standard. The *C. sanctus* and Green River fossil feathers give RDFs that are inconsistent with copper oxide or any other common mineral. (**B**) A comparison of the coordination chemistry of Cu in melanin to the fossil specimens (all distances to scale) showing similar coordination environments. (**C**) Proposed model for Cu complexation in fossil melanin: Cu coordination from EXAFS for *C. sanctus* is superimposed onto an optimized computational model of melanin (*20*), showing how Cu may be accommodated into eumelanin.

terpart of MGSF315 was completed to enable comparison of our synchrotron elemental mapping results with recent studies that have reconstructed pigmentation on the basis of structural analysis of proposed fossilized melanosomes. The Cu-rich neck sample showed some areas with elongate structures (Fig. 1H) that have been identified as fossilized eumelanosomes (*4*, *5*). The proximal flight feathers also showed these structures (fig. S4). Contrary to (*5*), we found no evidence of equant pheomelanosome structures in MGSF315 (or any other fossil), and so our results from this study pertain only to eumelanin. The sample taken from distal flight feathers with low Cu showed no structures that could be interpreted as melanosomes.

As shown in our elemental maps, Cu and other elements correlate with both macroscopic feather outlines and microscopic eumelanosome structures. These elements are either original to these fossils and reflect similar pigmentation in both of these specimens from the same taxa, or geochemical/geomicrobiological processes have acted posthumously on both, adding metals only to the feathers and preserving details of body and flight feathers.

Chemical spectroscopy suggests the patterning is probably endogenous. EXAFS analyses of copper oxide and copper melanin standards were compared with the flake sampled from the *C. sanctus* neck region and to a second fossil feather (BHI-6358) with high Cu zones (Fig. 2A). The strong backscattering from ordered second shell (and more distant) Cu atoms, which is diagnostic of copper oxide, is not present in the fossil feathers (figs. S5 to S8 and table S2). The radial distribution functions for *C. sanctus* and BHI-6358 are also inconsistent with other possible inorganic Cu phases, such as malachite [$Cu_2(OH)_2CO_3$ (*17*)], $Cu(OH)_2$ (*18*), or chalcopyrite [$CuFeS_2$; (*19*)]. In fact, the Cu-coordination chemistry in both fossils is predominantly an organic molecular compound (Fig. 2B) with coordination chemistry similar to Cu in natural eumelanin. The planar atoms of the *C. sanctus* Cu-coordination complex superimposed onto a recently optimized computational model of melanin (*20*) also indicates that the EXAFS data are consistent with Cu being sequestered within the channels of eumelanin or melanin-derived organic compounds (Fig. 2C). Copper bridging the edge carboxyl groups of two eumelanin fragments would also satisfy the EXAFS data (*21*). Thus, the trace metal detail shown in Fig. 1 is most likely derived from original eumelanin chelates in the feathers [supporting online material (SOM) text, fig. S9, and tables S3 and S4]. Unlike the *C. sanctus* feathers, BHI-6358 did not show melanosome-like structures via VP-FEG-SEM analysis. However, high-resolution XRF maps of BHI-6358 do show that Cu-enriched areas are aggregates of discrete patches 2 to 3 μm in size, which is consistent with original eumelanosome dimensions (figs. S4 and S10).

A range of additional fossil and extant organisms representing different geological conditions and various soft-tissue types were analyzed to test and constrain the *C. sanctus* results. Copper levels are elevated within the visibly darker regions of two Green River feathers (Fig. 3, H and I). Although BHI-6358 did not preserve any detectable melanosomes, SEM analysis did reveal fossilized eumelanosomes within Cu-enriched areas of the feather exposed within BHI-6319 (fig. S4). The eye of the fossil fish in specimen BHI-6319 also shows elevated Cu levels (Fig. 3J), but traces of melanosomes in the fish eye could not be resolved. Eyes in extant fish have been shown to contain high

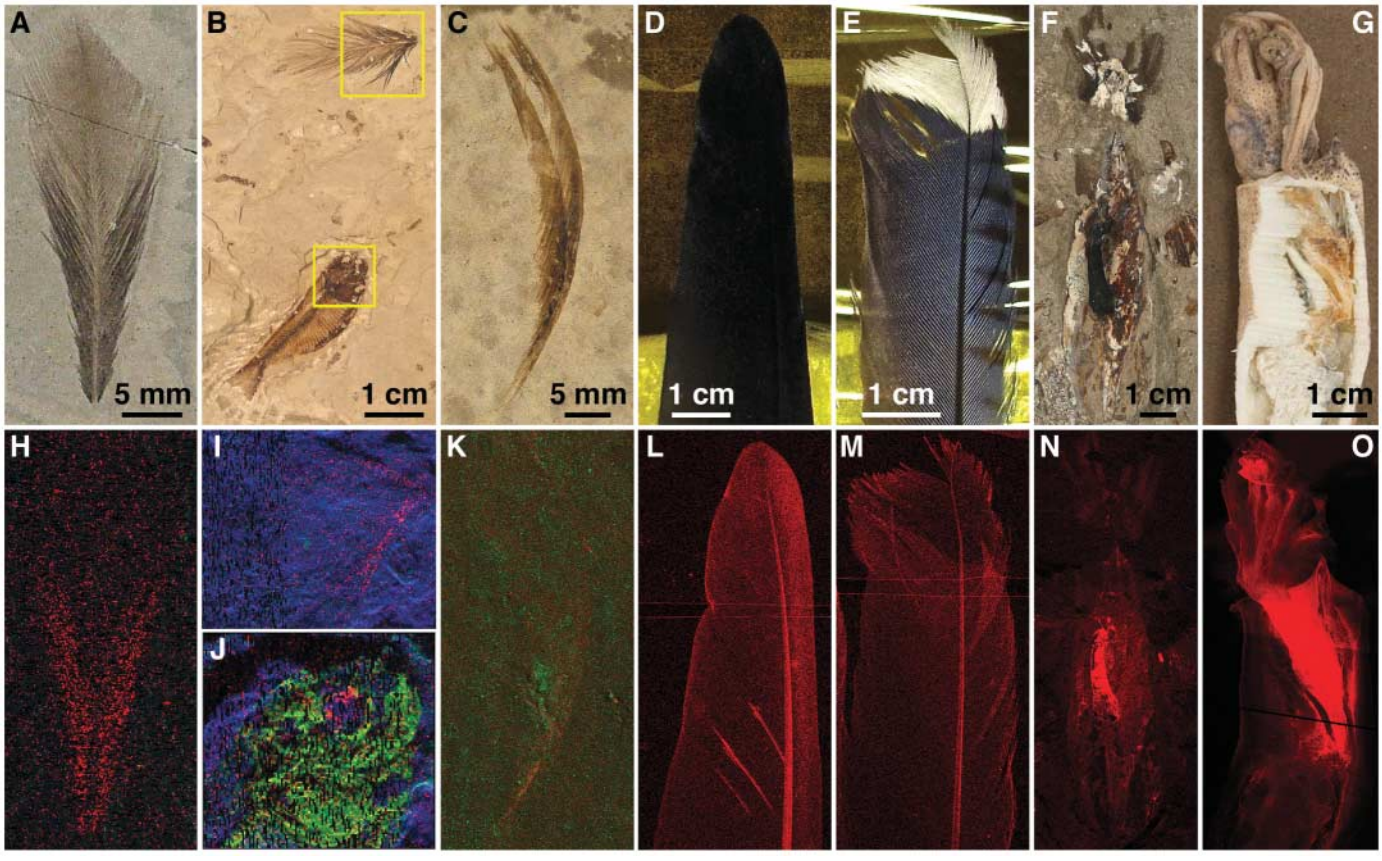

Fig. 3. (**A** to **G**) optical images and (**H** to **O**) SRS-XRF false-color images of [(A) and (H)] Green River fossil feather BHI-6358, [(B), (I), and (J)] Green River fossil feather and fish BHI-6319, [(C) and (K)] *G. yumenensis* fossil feather MGSF317, [(D) and (L)] eagle feather, [(E) and (M)] blue jay feather, [(F) and (N)] Hakel fossil squid BHI-2243B, and [(G) and (O)] sectioned extant squid. For BHI-6358 and BHI-6319, red, Cu; green, Ca; and blue, Fe. For MGSF317, red, Cu; and green, Ca. For the remaining images, red, Cu. All have Cu zonation controlled by biological structure, indicating eumelanin pigmentation.

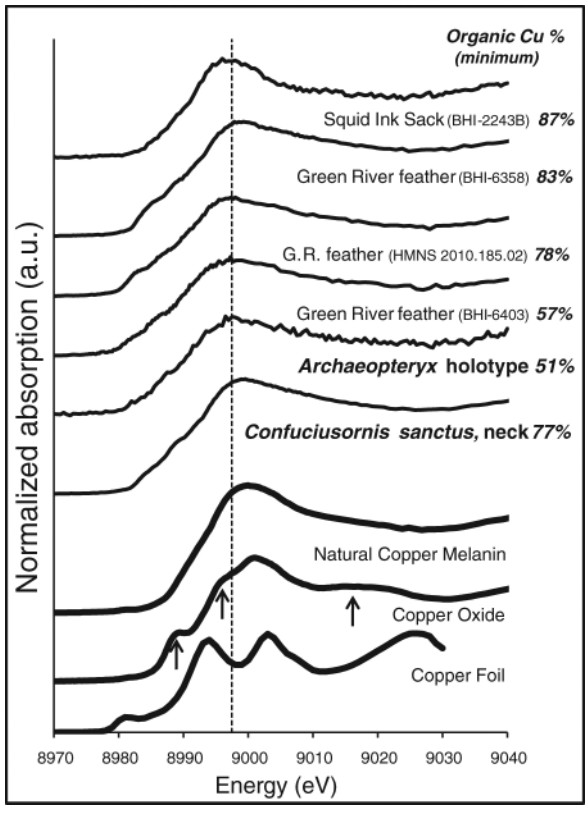

Fig. 4. XANES spectra at the Cu K edge for three standards (thick black lines indicate Cu metal foil, copper oxide, and natural melanin with high Cu content) and six fossil specimens [*C. sanctus* neck (MGSF315), *A. lithographica* (MB.Av.100), three individual feather samples from the Green River Formation (BHI-6358, HMNS 2010.185.02, and BHI-6403), and a fossilized squid ink sack from the Hakel Formation, *S. officinalis* (BHI-2243B)]. Arrows on the copper oxide spectrum indicate spectral features that do not appear on the eumelanin standard or on the fossils. The vertical dashed line indicates the fossils' average spectral maximum. Minimum organic Cu content within the fossils as calculated with linear combination analysis is shown by values at right of each spectrum.

concentrations of melanin-related Cu (*22*). A lone *Gansus yumenensis* feather (MGSF317) displays areas of elevated trace copper (Fig. 3K) and these areas are correlated with preserved eumelanosome structures (fig. S4). Crucially, SRS-XRF maps of extant feathers show a correlation between pigment density and trace Cu (Fig. 3, L and M). Lastly, results from both fossil (Fig. 3N) and extant squid (Fig. 3O) show that high Cu concentrations correlate with the eumelanin-rich ink sack regions (*23*, *24*). All of these maps are consistent with the proposed spatial correlation between original eumelanin pigmentation and Cu.

XANES spectra, which are sensitive to the electronic structure of the probed central absorber atom, were acquired from several standards and fossil specimens. Three Green River feather specimens, a fossil squid, and the *C. sanctus* fossil all produced Cu XANES spectra that resemble the extant *Sepia officinalis* eumelanin standard (Fig. 4). This also holds for the Cu XANES taken from the holotype of *A. lithographica*, suggesting that the residue of melanin pigmentation patterns is present even within one of the earliest avian ancestors. Linear combination shows that organic complexes represent the majority of the Cu inventory in all of these fossils (Fig. 4, figs. S11 and S12, and table S5). These results agree with the Cu/melanin correlation observed in *C. sanctus* and suggest that trace element chemistry provides a robust and consistent method for identifying pigment because metal zoning may be preserved long after melanosome structures have been destroyed, as in BHI-6358. Additionally, infrared spectral analysis shows that the organic functional groups in *C. sanctus*, BHI-6358, and several of the other fossil feathers have a strong eumelanin affinity and a distribution pattern that is controlled by soft-tissue residue, which is similar to recent results with fossil skin (figs. S13 to S15 and table S6) (*25*).

Trace metals in *C. sanctus* are high in the downy feathers. Metal concentrations gradationally reduce within the proximal flight feathers but show patchy regions of higher concentration near the tips, indicating lighter bands in the proximal flight feathers. A lack of trace metals in the distal flight feathers suggests that these were not eumelanin-rich, and the lack of preserved melanosomes argues against pheomelanosome pigmentation. Distal flight feathers therefore were either mostly white or colored by another mechanism, such as carotenoids. This suggests that *C. sanctus* most probably had darkly shaded regions, with the most intense eumelanin pigmentation in the downy body feathers and in the lengthy retrices (Fig. 1I).

References and Notes

1. J. D. Simon, D. Peles, K. Wakamatsu, S. Ito, *Melanoma Res.* **22**, 563 (2009).
2. L. H. Hou, L. D. Martin, Z. H. Zhou, A. Feduccia, F. C. Zhang, *Nature* **399**, 679 (1999).
3. H. L. You *et al.*, *Science* **312**, 1640 (2006).
4. F. C. Zhang *et al.*, *Nature* **463**, 1075 (2010).
5. Q. Li *et al.*, *Science* **327**, 1369 (2010).
6. B. H. Willier, M. E. Rawles, *Physiol. Zool.* **13**, 177 (1940).
7. C. L. Ralph, *Am. Zool.* **9**, 521 (1969).
8. J. A. Clarke *et al.*, *Science* **330**, 954 (2010).
9. A. Palumbo, M. d'Ischia, G. Misuraca, G. Prota, T. M. Schultz, *Biochim. Biophys. Acta* **964**, 193 (1988).
10. B. S. Larsson, *Pigment Cell Res.* **6**, 127 (1993).
11. K. J. McGraw, *Oikos* **102**, 402 (2003).
12. M. Niecke, M. Heid, A. Kruger, *J. Ornithol.* **140**, 355 (1999).
13. Materials and methods are available as supporting material on *Science* Online.
14. U. Bergmann *et al.*, *Proc. Natl. Acad. Sci. U.S.A.* **107**, 9060 (2010).
15. M. Katsikini, E. Mavromati, F. Pinakidou, E. C. Paloura, D. Gioulekas, *J. Phys. Conf. Ser.* **190**, 012204 (2009).
16. K. J. McGraw, in *Bird Coloration*, G. E. Hill, K. J. McGraw, Eds. (Harvard Univ. Press, Cambridge, MA, 2006), vol. 1, chap. 6.
17. A. I. Frenkel, G. V. Korshin, *J. Synchrotron Radiat.* **6**, 653 (1999).
18. S.-F. Cheah, G. E. Brown Jr., G. A. Parks, *Am. Mineral.* **85**, 118 (2000).
19. G. R. Helz, J. M. Charnock, D. J. Vaughan, C. D. Garner, *Geochim. Cosmochim. Acta* **57**, 15 (1993).
20. E. Kaxiras, A. Tsolakidis, G. Zonios, S. Meng, *Phys. Rev. Lett.* **97**, 218102 (2006).
21. J. Stainsack *et al.*, *Inorg. Chim. Acta* **356**, 243 (2003).
22. J. M. Bowness, R. A. Morton, *Biochem. J.* **51**, 530 (1952).
23. Y. Liu *et al.*, *Pigment Cell Res.* **17**, 262 (2004).
24. Y. Liu, J. D. Simon, *Pigment Cell Res.* **16**, 72 (2003).
25. N. P. Edwards *et al.*, *Proc. R. Soc. B*, published online 23 March 2011 (10.1098/rspb.2011.0135).

Acknowledgments: Samples were provided by the Black Hills Institute Museum and the Museum für Naturkunde, Humboldt University, Berlin. We thank D. Schwarz-Wings for making the *Archaeopteryx* sample available. We also thank Perkin-Elmer, M. George, K. Palmer, E. Kaxiras, V. Vishnyakov, and R. Morton for technical assistance and additional data, and D. Vaughan, G. Brown, and three reviewers for helpful comments on the manuscript. Portions of this research were carried out at SSRL, a national user facility operated by Stanford University on behalf of the U.S. Department of Energy, Office of Basic Energy Sciences. Funding was provided in part by a Natural Environment Research Council Envirosync grant and by an anonymous private donor. R. Hartley provided the artist's drawing of *C. sanctus*. Data described in this paper are presented within the SOM. R.A.W. wrote the manuscript, analyzed the data, and supervised or assisted in all analyses. P.L.M. cowrote the manuscript and assisted in all analyses. H.E.B., N.P.E., and W.I.S. assisted in all analyses and contributed to the manuscript. S.M.W. performed the EXAFS analyses. K.G.T. provided and supervised VP-FEG-SEM analyses. P.L.L. provided specimen access and identification and also assisted with all x-ray measurements. P.D. consulted on the manuscript, and along with H.Y. and L.D. assisted in field collection, preparation, and identification of samples. U.B. supervised the SRS-XRF program and assisted in manuscript preparation.

Supporting Online Material

www.sciencemag.org/cgi/content/full/science.1205748/DC1
Materials and Methods
SOM Text
Figs. S1 to S15
Tables S1 to S6
References (*26*–*38*)

17 March 2011; accepted 2 June 2011
Published online 30 June 2011;
10.1126/science.1205748